

## Bright-dark soliton complexes in spinor Bose-Einstein condensates

H. E. Nistazakis,<sup>1</sup> D. J. Frantzeskakis,<sup>2</sup> P. G. Kevrekidis,<sup>2</sup> B. A. Malomed,<sup>3</sup> and R. Carretero-González<sup>4</sup>

<sup>1</sup>*Department of Physics, University of Athens, Panepistimiopolis, Zografos, Athens 15784, Greece*

<sup>2</sup>*Department of Mathematics and Statistics, University of Massachusetts, Amherst, Massachusetts 01003-4515, USA*

<sup>3</sup>*Department of Physical Electronics, Faculty of Engineering, Tel Aviv University, Tel Aviv 69978, Israel*

<sup>4</sup>*Nonlinear Dynamical Systems Group\*, Department of Mathematics and Statistics, and Computational Science Research Center, San Diego State University, San Diego, California 92182-7720, USA*

(Received 2 January 2008; published 13 March 2008)

We consider vector solitons of mixed bright-dark types in quasi-one-dimensional spinor ( $F=1$ ) Bose-Einstein condensates. Using a multiscale expansion technique, we reduce the corresponding nonintegrable system of three coupled Gross-Pitaevskii equations (GPEs) to an integrable Yajima-Oikawa system. In this way, we obtain approximate solutions for small-amplitude vector solitons of dark-dark-bright and bright-bright-dark types, in terms of the  $m_F=+1, -1, 0$  spinor components, respectively. By means of numerical simulations of the full GPE system, we demonstrate that these states indeed feature soliton properties, i.e., they propagate undistorted and undergo quasielastic collisions. It is also shown that in the presence of a parabolic trap the bright component(s) is (are) guided by the dark one(s) and, as a result, the small-amplitude vector soliton as a whole performs quasiharmonic oscillations. The oscillation frequency is found as a function of the spin-dependent interaction strength for both small-amplitude and large-amplitude solitons.

DOI: [10.1103/PhysRevA.77.033612](https://doi.org/10.1103/PhysRevA.77.033612)

PACS number(s): 03.75.Mn, 05.45.Yv

### I. INTRODUCTION

The development of far-off-resonant optical techniques for trapping of ultracold atomic gases has opened new directions in the studies of Bose-Einstein condensates (BECs), allowing one to confine atoms regardless of their spin (hyperfine) state; see, e.g., Ref. [1]. One of major achievements in this direction was the experimental creation of spinor BECs [2,3], in which the spin degree of freedom (frozen in magnetic traps) comes into play. This gave rise to the observation of various phenomena that are not present in single-component BECs, including formation of spin domains [4] and spin textures [5].

A spinor condensate formed by atoms with spin  $F$  is described by a macroscopic wave function with  $(2F+1)$  components. Accordingly, a number of theoretical works have been dealing with multicomponent (vector) solitons in  $F=1$  spinor BECs. Bright [6–8] and dark [9] solitons, as well as gap solitons [10], have been predicted in this context (the latter type requires the presence of an optical lattice). However, mixed vector soliton solutions, composed of bright and dark components, of the respective system of coupled Gross-Pitaevskii equations (GPEs) have not been reported yet, to the best of our knowledge. Actually, compound solitons of the mixed type may be of particular interest, as they would provide for the possibility of all-matter-wave waveguiding, with the dark soliton component building an effective conduit for the bright component, similar to the all-optical waveguiding proposed in nonlinear optics [11]. Waveguides of this kind would be useful for applications, such as quantum switches and splitters emulating their optical counterparts [12].

On the other hand, mixed solitons of the dark-bright type were considered in a model of a two-component condensate,

described by two coupled GPEs [13]. Actually, the model also assumed that the two components represented different spin states of the same atomic species, with equal scattering lengths of the intracomponent and intercomponent atomic collisions (i.e., the matrix of the nonlinear coefficients in the coupled GPEs was of the Manakov type [14], which makes the system integrable in the absence of an external potential).

In this work we consider a quasi-one-dimensional (quasi-1D) spinor condensate with  $F=1$ , described by a system of three coupled GPEs. In the physically relevant case of  $^{87}\text{Rb}$  and  $^{23}\text{Na}$  atoms with  $F=1$ , which are known to form spinor condensates of ferromagnetic and polar types, respectively (the definitions are given below), the system includes a naturally occurring small parameter  $\delta$ , namely, the ratio of the strengths of the spin-dependent and spin-independent interatomic interactions [15,16]. In the case of  $\delta=0$  and without the external potential, the system of the three coupled GPEs also belongs to the above-mentioned Manakov's type [14], i.e., it is integrable [17], thus bearing many similarities to the system considered in Ref. [13]. Exploiting the smallness of  $\delta \neq 0$ , we will develop a multiscale expansion method to asymptotically reduce the nonintegrable GPE system to another integrable one, viz., the Yajima-Oikawa (YO) system. The latter one was originally derived to describe the interaction of Langmuir and sound waves in plasmas [18] and has been used in studies of vector solitons in the context of optics [19] and binary BECs [20]. The asymptotic reduction is valid for homogeneous polar spinor BECs (such as  $^{23}\text{Na}$ ), that are not subject to the modulational instability [7,21]. Borrowing exact soliton solutions from the YO system, we predict two types of vector-soliton complexes in the spinor condensate, viz., dark-dark-bright (DDB) and bright-bright-dark (BBD) ones for the  $m_F=+1, -1, 0$  spin components, respectively. Numerical simulations of the underlying (full) GPE system show that these solitary pulses (including ones with moderate rather than small amplitudes) emulate solitons

\*<http://nlds.sdsu.edu/>

in integrable systems quite well. In fact, we find that the solitons propagate undistorted for a long time, and undergo quasielastic collisions (quasielastic collisions of solitons in the nonintegrable two-component system were mentioned earlier in Ref. [13]).

The effect of the harmonic trapping potential (of strength  $\omega$ ) on the solitons is also studied in this work, analytically and numerically (the potential breaks the exact integrability of the coupled GPE equations, even with  $\delta=0$ ). First we confine ourselves in the case of the small normalized spin-dependent interaction strength  $\delta \sim 10^{-2}$  (note that the  $^{23}\text{Na}$  spinor BEC has  $\delta=0.0314$ ). It is shown that, regardless of their amplitude, the vector solitons of the mixed types perform quasiharmonic oscillations in the presence of the trap, and we find their oscillation frequency as a function of the trap's strength  $\omega$ . In particular, we at first study the case of small-amplitude vector solitons, and quantitatively estimate the deviations from the results pertaining to one- or two-component cases arising due to the spin-dependent interactions (i.e., for nonzero  $\delta$ ). Specifically, we develop a local density approximation to show that, for  $\delta=0$ , the oscillation frequency is  $\omega/\sqrt{2}$ , which, in the appropriate limits, coincides with the well-known frequency of oscillations of a dark soliton in the single-component [22,23] or two-component [13] BECs. Moreover, for  $\delta \neq 0$ , we develop a semianalytical approach to determine the oscillation frequency as a function of  $\delta$  and find that the respective correction to the frequency is negative, and scales as  $-\sqrt{\delta}$ . The oscillations of the vector soliton with moderate and large amplitudes are studied as well, the oscillation frequency getting down-shifted from its value pertaining to small-amplitude solitons as the depth of the dark component of the vector soliton increases. In the case of large-amplitude solitons that perform small-amplitude oscillations around the trap's center, the frequency down-shift is well approximated by the prediction reported, for  $\delta=0$ , in Ref. [13]. For this case, we also find a small deviation from that prediction, for  $\delta \neq 0$ , which is essentially weaker than in the above-mentioned case of the small-amplitude solitons, scaling as  $-\delta^2$ . In all cases, the bright component(s) of the vector soliton follow their dark counterpart(s), oscillating at the same frequency (ordinary bright solitons in the single-component BEC oscillate simply at frequency  $\omega$  [24], according to Kohn's theorem [25]). As a matter of fact, this effect is a manifestation of the guidance of the bright component by the dark one.

We also investigate the effect of a larger normalized spin-dependent interaction strength  $\delta$  on the stability of the vector solitons. To highlight these effects, we take  $\delta$  an order of magnitude larger than its actual value for the polar sodium spinor condensate ( $\delta=0.2$  rather than  $\sim 10^{-2}$ ), and solve the respective coupled GPEs numerically. The result is that, generally, under such a strong perturbation the solitons emit radiation at a conspicuous rate, and are eventually destroyed. However, even for large  $\delta$ , small- and moderate-amplitude DDB solitons persist up to relatively large times,  $\geq 300$  ms in physical units. Given that for the physically relevant small value of  $\delta$ , which pertains to the sodium spinor BEC, the respective lifetime is four times as large, we believe that the vector solitons predicted in this work have a good chance to be observed experimentally.

The paper is organized as follows. In Sec. II we present the model, expound our analytical approach for the homogeneous system, and derive solutions for the bright-dark soliton complexes. Section III presents numerical and analytical results for the dynamics of the solitons in both the homogeneous and inhomogeneous (harmonically confined) media. Finally, Sec. IV concludes the paper.

## II. THE MODEL AND ITS ANALYTICAL CONSIDERATION

### A. The model

At sufficiently low temperatures (finite-temperature effects have been considered recently in Ref. [26]) and in the framework of the mean-field approach, the spinor BEC with  $F=1$  is described by the vector order parameter  $\Psi(\mathbf{r},t) = [\Psi_{-1}(\mathbf{r},t), \Psi_0(\mathbf{r},t), \Psi_{+1}(\mathbf{r},t)]^T$ , with the components corresponding to the three values of the vertical spin component  $m_F = -1, 0, +1$ . Assuming that the condensate is kept in a highly anisotropic trap, with the longitudinal and transverse trapping frequencies chosen so that  $\omega_x \ll \omega_\perp$ , we may assume approximately separable wave functions  $\Psi_{0,\pm 1} \approx \psi_{0,\pm 1}(x)\psi_\perp(y,z)$ , where  $\psi_\perp(y,z)$  is the ground state of the respective harmonic oscillator. Then, averaging of the underlying system of the coupled three-dimensional (3D) GPEs in the transverse plane ( $y,z$ ) [27] leads to the following system of coupled 1D equations for the longitudinal components of the wave functions (see also Refs. [6–10]):

$$i\hbar\partial_t\psi_{\pm 1} = \mathcal{H}_0\psi_{\pm 1} + c_2^{(1D)}(|\psi_{\pm 1}|^2 + |\psi_0|^2 - |\psi_{\mp 1}|^2)\psi_{\pm 1} + c_2^{(1D)}\psi_0^2\psi_{\mp 1}^*, \quad (1)$$

$$i\hbar\partial_t\psi_0 = \mathcal{H}_0\psi_0 + c_2^{(1D)}(|\psi_{-1}|^2 + |\psi_{+1}|^2)\psi_0 + 2c_2^{(1D)}\psi_{-1}\psi_0^*\psi_{+1}, \quad (2)$$

where the asterisk denotes the complex conjugate and  $\mathcal{H}_0 \equiv -(\hbar^2/2m)\partial_x^2 + (1/2)m\omega_x^2x^2 + c_0^{(1D)}n_{\text{tot}}$  is the spin-independent part of the effective Hamiltonian, with  $n_{\text{tot}} = |\psi_{-1}|^2 + |\psi_0|^2 + |\psi_{+1}|^2$  being the total density ( $m$  is the atomic mass). The nonlinearity coefficients have an effectively 1D form, namely,  $c_0^{(1D)} = c_0/2\pi a_\perp^2$  and  $c_2^{(1D)} = c_2/2\pi a_\perp^2$ , where  $a_\perp = \sqrt{\hbar/m\omega_\perp}$  is the transverse harmonic oscillator length, which defines the size of the transverse ground state. Coupling constants  $c_0$  and  $c_2$  which account, respectively, for the spin-independent and spin-dependent interactions between identical spin-1 bosons, are (in the mean-field approximation)

$$c_0 = \frac{4\pi\hbar^2(a_0 + 2a_2)}{3m}, \quad c_2 = \frac{4\pi\hbar^2(a_2 - a_0)}{3m}, \quad (3)$$

where  $a_0$  and  $a_2$  are the  $s$ -wave scattering lengths in the symmetric channels with total spin of the colliding atoms  $F=0$  and  $F=2$ , respectively. Note that the  $F=1$  spinor condensate may be either ferromagnetic (such as the  $^{87}\text{Rb}$ ), characterized by  $c_2 < 0$ , or polar (such as the  $^{23}\text{Na}$ ), with  $c_2 > 0$  [28,29].

Measuring time, length, and density in units of  $\hbar/c_0^{(1D)}n_0$ ,  $\hbar/\sqrt{mc_0^{(1D)}}n_0$ , and  $n_0$ , respectively (where  $n_0$  is the peak den-

sity), we cast Eqs. (1) and (2) in the dimensionless form

$$i\partial_t\psi_{\pm 1} = H_0\psi_{\pm 1} + \delta[|\psi_{\pm 1}|^2 + |\psi_0|^2 - |\psi_{\mp 1}|^2]\psi_{\pm 1} + \delta\psi_0^2\psi_{\mp 1}^*, \quad (4)$$

$$i\partial_t\psi_0 = H_0\psi_0 + \delta[|\psi_{-1}|^2 + |\psi_{+1}|^2]\psi_0 + 2\delta\psi_{-1}\psi_0^*\psi_{+1}, \quad (5)$$

where  $H_0 \equiv -(1/2)\partial_x^2 + (1/2)\Omega_{\text{tr}}^2x^2 + n_{\text{tot}}$ , the normalized trap's strength is

$$\Omega_{\text{tr}} = \frac{3}{2(a_0 + 2a_2)n_0} \left( \frac{\omega_x}{\omega_{\perp}} \right) \quad (6)$$

and we define

$$\delta \equiv \frac{c_2^{(1D)}}{c_0^{(1D)}} = \frac{a_2 - a_0}{a_0 + 2a_2}. \quad (7)$$

According to what was said above,  $\delta < 0$  and  $\delta > 0$  correspond, respectively, to ferromagnetic and polar spinor BECs. In the relevant cases of  $^{87}\text{Rb}$  and  $^{23}\text{Na}$  atoms with  $F=1$ , this parameter takes values  $\delta = -4.66 \times 10^{-3}$  [15] and  $\delta = +3.14 \times 10^{-2}$  [16], respectively, i.e., in either case, it is a small parameter in Eqs. (4) and (5).

Equations (4) and (5) may give rise to both spin-mixing [30] and spin-polarized states [28,31]. Here, we first consider the spatially homogeneous system ( $\Omega_{\text{tr}}=0$ ), and focus on solutions having at least one component equal to zero, the remaining ones being continuous waves (CWs). The corresponding exact stationary solutions are

$$\psi_{-1} = \psi_{+1} = \sqrt{\frac{\mu}{2}} \exp(-i\mu t), \quad \psi_0 = 0, \quad (8)$$

$$\psi_{-1} = \psi_{+1} = 0, \quad \psi_0 = \sqrt{\mu} \exp(-i\mu t). \quad (9)$$

As we demonstrate below, small perturbations around solutions (8) and (9) may lead to the formation of three-component dark-bright soliton complexes of the DDB and BBD types, respectively, in terms of components  $\psi_{\pm 1}$  and  $\psi_0$ . Since the analytical approach and the derivation of the soliton solutions for the two cases are quite similar, we focus below on the DDB solitons, and discuss the BBD ones only briefly.

It is relevant to note that, for solutions with  $\psi_{+1} = \psi_{-1} \equiv \psi_1$ , Eqs. (4) coalesce into a single one for the wave function  $\psi_1$ . Then, the transformation  $\psi_1 \equiv (\phi_D + \phi_B)/(2\sqrt{1+\delta^2})$ ,  $\psi_0 \equiv (\phi_D - \phi_B)/\sqrt{1+\delta^2}$  casts the system of two Eqs. (4) and (5) into the form of two coupled GPEs, with nonlinear cross-coupling coefficients  $g_D = g_B = (1-\delta)/(1+\delta)$ , which was introduced in Ref. [13] with the objective to study bound complexes of dark-bright solitons, carried by fields  $\phi_D$  and  $\phi_B$ , respectively. In fact, the analytical results of Ref. [13] were basically referring to the case of  $g_D = g_B = 1$ , while deviations from this (Manakov's) limit were also briefly discussed, and numerical results for soliton collisions with  $\delta \neq 0$  were presented. In this work, we focus on effects generated by spin-dependent interactions, i.e., for small  $\delta \neq 0$ . It should also be stressed that, although stationary equations presented below may indeed be found from the system of two, rather than three, coupled GPEs, stability

tests for the solutions are performed against general perturbations (see below), which include those with  $\psi_{+1} \neq \psi_{-1}$  (i.e., the full system of the three equations was employed in the direct numerical simulations).

## B. Linear analysis

Aiming to find solutions of Eqs. (4) and (5) close to the CW solution given by Eq. (8), we start the analysis by adopting the following ansatz:

$$\begin{aligned} \psi_{-1} = \psi_{+1} &= \sqrt{n(x,t)} \exp[-i\mu t + i\phi(x,t)], \\ \psi_0 &= \Phi_0(x,t) \exp(-i\mu t), \end{aligned} \quad (10)$$

where  $n(x,t)$  and  $\phi(x,t)$  are real and represent the density and phase of fields  $\psi_{\pm 1}$ , while  $\Phi_0$  is, generally, a complex function. Substituting Eq. (10) into Eqs. (4) and (5), we derive the following system:

$$\begin{aligned} \frac{i}{2} [\partial_t n + \partial_x(n\partial_x\phi)] - n[\partial_t\phi + 2n - \mu + (1+\delta)|\Phi_0|^2] \\ - n \left[ \frac{1}{2}(\partial_x\phi)^2 - \frac{1}{2\sqrt{n}}\partial_x^2\sqrt{n} + \delta\Phi_0^2 e^{-2i\phi} \right] = 0, \end{aligned} \quad (11)$$

$$i\partial_t\Phi_0 + \frac{1}{2}\partial_x^2\Phi_0 - (2n - \mu + |\Phi_0|^2)\Phi_0 - 2\delta n(\Phi_0 + \Phi_0^* e^{-2i\phi}) = 0. \quad (12)$$

The CW state (8) corresponds to an obvious solution of Eqs. (11) and (12) with  $n = \mu/2$ ,  $\phi = 0$ ,  $\Phi_0 = 0$ . Next, we linearize the equations around this state, looking for a solution as  $n = (\mu/2) + \epsilon\tilde{n}$ ,  $\phi = \epsilon\tilde{\phi}$ , and  $\Phi_0 = \epsilon\tilde{\Phi}_0$ , where  $\epsilon$  is a formal small parameter. At order  $O(\epsilon)$ , the linearization leads to the following system:

$$i \left( \partial_t\tilde{n} + \frac{\mu}{2}\partial_x^2\tilde{\phi} \right) - \mu \left( \partial_t\tilde{\phi} + 2\tilde{n} - \frac{\mu}{4}\partial_x^2\tilde{n} \right) = 0, \quad (13)$$

$$i\partial_t\tilde{\Phi}_0 + \frac{1}{2}\partial_x^2\tilde{\Phi}_0 - \delta\mu(\tilde{\Phi}_0 + \tilde{\Phi}_0^*) = 0. \quad (14)$$

Combining real and imaginary parts of Eq. (13), we arrive at a dispersive wave equation

$$\partial_t^2\tilde{n} - \mu\partial_x^2\tilde{n} + (\mu^2/8)\partial_x^4\tilde{n} = 0, \quad (15)$$

which gives rise to a stable dispersion relation between wave number  $k$  and frequency  $\omega$  (the absence of complex roots for  $\omega$  at real  $k$  implies the modulational stability of the underlying CW state):

$$\omega^2 = \mu k^2(1 + \mu k^2/8). \quad (16)$$

It follows from Eq. (16) that, in the long-wave limit ( $k \rightarrow 0$ ), small-amplitude waves can propagate on top of CW solution (8) with the speed of sound

$$c = \sqrt{\mu}. \quad (17)$$

A similar analysis for Eq. (14), which is decoupled from Eq. (13), leads to the dispersion relation

$$\omega^2 = k^2(\delta \cdot \mu + k^2/4). \quad (18)$$

It is clear from here that, for  $\delta > 0$  (which corresponds to the polar state), Eq. (18) has no complex roots for  $\omega$ , hence the trivial solution to Eq. (12),  $\Phi_0=0$ , is modulationally stable. However,  $\delta < 0$  (corresponding to the ferromagnetic state) gives rise to modulational instability of the  $\Phi_0=0$  solution against the perturbations whose wave numbers belong to the instability band  $k \leq 2\sqrt{|\delta|\mu}$ . Note that these results comply with those reported in Ref. [21]. Below, we focus on the modulationally stable case, which pertains to the polar state with  $\delta > 0$ .

### C. Asymptotic soliton solutions

We now consider solutions for small deviations from the CW state. Recalling that  $\delta$  is a small parameter, we introduce the stretched variables in Eqs. (4) and (5),

$$X \equiv \sqrt{\delta}(x - \sqrt{\mu}t), \quad T \equiv \delta t. \quad (19)$$

Then, we seek for solutions to Eqs. (11) and (12) as

$$n = (\mu/2) + \delta\rho, \quad \phi = \sqrt{\delta}\alpha, \quad \Phi_0 = \delta^{3/4}q, \quad (20)$$

$$q \equiv q_1 \cos(Kx - \Omega t) + iq_2 \sin(Kx - \Omega t), \quad (21)$$

where  $\rho = \rho(X, T)$ ,  $\alpha = \alpha(X, T)$ ,  $q_{1,2} = q_{1,2}(X, T)$ , while  $K$  and  $\Omega$  are unknown wave number and frequency. Substituting Eq. (20) in Eq. (11) at order  $O(\delta)$ , we derive a relation between density  $\rho$  and phase  $\alpha$ ,

$$\sqrt{\mu}\partial_X\alpha = 2\rho. \quad (22)$$

On the other hand, at order  $O(\delta^{3/2})$ , the resulting equation is complex:

$$-(i\mu/4)(2\partial_X\bar{\rho} - \sqrt{\mu}\partial_X^2\alpha) + \partial_T\alpha + |q|^2 = 0. \quad (23)$$

The imaginary part of the expression on the left-hand side of Eq. (23) vanishes due to the validity of Eq. (22), while the real part leads to equation  $\partial_T\alpha + |q|^2 = 0$ . The condition for its compatibility with Eq. (22) is

$$\partial_T\rho = -(\sqrt{\mu}/2)\partial_X(|q|^2). \quad (24)$$

We now proceed to Eq. (12), which, to leading order in  $\delta$ , i.e., at  $O(\delta^{3/4})$ , yields the following system:

$$\Omega q_1 - (K^2/2)q_2 = 0, \quad -[(K^2/2) + 2\mu]q_1 + \Omega q_2 = 0. \quad (25)$$

Nontrivial solutions to Eqs. (25) are possible when the following dispersion relation for  $\Omega$  and  $K$  holds:

$$\Omega^2 = K^2(\mu + K^2/4). \quad (26)$$

Next, to order  $O(\delta^{5/4})$ , Eq. (12) leads to a system

$$-\sqrt{\mu}\partial_X q_1 + K\partial_X q_2 = 0, \quad -K\partial_X q_1 + \sqrt{\mu}\partial_X q_2 = 0,$$

which has nontrivial solutions if  $K^2 = \mu$ . In combination with Eq. (26), the latter relation selects the frequency,  $\Omega = 5\mu^2/4$ . Finally, at order  $O(\delta^{7/4})$ , Eq. (12) leads to equation

$$i\partial_T q + \frac{1}{2}\partial_X^2 q - 2\rho q = 0. \quad (27)$$

Equations (24) and (27), which are the basic result of our analysis, constitute the Yajima-Oikawa (YO) system. It describes the interaction of low- and high-frequency waves, and was originally derived in the context of plasma physics; in this context, it applies to Langmuir (high-frequency) waves, which form a wave packet (soliton) moving at velocities close to the speed of sound, and are thus strongly coupled to the ion-acoustic (low-frequency) waves [18]. As shown in Ref. [18], the YO system is integrable by means of the inverse-scattering transform, and gives rise to soliton solutions. The solitons have the  $-\text{sech}^2$  shape for field  $\rho$ , and  $\text{sech}$  shape for  $q$ , which correspond to a density dip for components  $\psi_{\pm 1}$  and a bright soliton for  $\psi_0$ , as per Eqs. (20). According to Eq. (22), the phase profile of the  $\psi_{\pm 1}$  components, in the form of  $\tanh$ , is associated to the density dip, hence the patterns in these components, generated by the exact solution of the YO system, are dark solitons. The full form of the approximate (asymptotic) DDB soliton solution to Eqs. (4) and (5), into which the YO soliton is mapped by Eqs. (10), (19), and (20), is

$$\psi_{\pm 1}(x, t) = \sqrt{(\mu/2) - 2\delta\eta^2 \text{sech}^2(2\sqrt{\delta}\eta Z)} \\ \times \exp[-i\mu t - 2i\eta\sqrt{\delta\mu} \tanh(2\sqrt{\delta}\eta Z)], \quad (28)$$

$$\psi_0(x, t) = 2^{3/2}\delta^{3/4}\eta\mu^{-1/4}\sqrt{\xi} \text{sech}(2\sqrt{\delta}\eta Z) \\ \times \exp[-i\mu t + i\sqrt{\mu}x - 2i\sqrt{\delta}\xi Z + 2i\delta(\eta^2 - \xi^2)t], \quad (29)$$

where  $Z \equiv x - (\sqrt{\mu} - 2\sqrt{\delta}\xi)t$ , while  $\eta$  and  $\xi$  are arbitrary parameters of order  $O(1)$ .

A similar analysis can be performed to derive asymptotic soliton solutions of the BBD type. In that case, starting from CW solution (9), we seek for solutions of Eqs. (4) and (5) in the form of

$$\psi_{-1} = \psi_{+1} = \Phi_0(x, t)\exp(-i\mu t), \quad (30)$$

$$\psi_0 = \sqrt{n(x, t)}\exp[-i\mu t + i\phi(x, t)].$$

Next, following the same analytical approach which has led above to the DDB soliton, we again end up with the YO system, in a form similar to Eqs. (24) and (27):

$$\partial_T\rho = -2\sqrt{\mu}\partial_X|q|^2, \quad i\partial_T q + \frac{1}{2}\partial_X^2 q - \rho q = 0. \quad (31)$$

Eventually, the approximate BBD soliton solution to Eqs. (4) and (5), generated by the YO soliton, is

$$\psi_{\pm 1}(x, t) = 2\delta^{3/4}\eta\mu^{-1/2}\sqrt{\xi} \text{sech}(2\sqrt{\delta}\eta Z) \\ \times \exp[-i\mu t + i\sqrt{\mu}x - 2i\sqrt{\delta}\xi Z + 2i\delta(\eta^2 - \xi^2)t], \quad (32)$$

$$\psi_0(x,t) = \sqrt{(\mu/2) - 4\delta\eta^2 \operatorname{sech}^2(2\sqrt{\delta}\eta Z)} \\ \times \exp[-i\mu t - 2i\eta\sqrt{\delta/\mu} \tanh(2\sqrt{\delta}\eta Z)]. \quad (33)$$

As the latter solution is quite similar to the DDB one, given by Eqs. (28) and (29), below we only deal with the dynamics of the DDB solitons. It is worthwhile to note in passing that both types of solutions are genuinely traveling ones, i.e., they do not exist with zero speed.

### III. DYNAMICS OF DARK-DARK-BRIGHT SPINOR SOLITONS

#### A. Numerical results

In order to test the prediction of the existence of the DDB solitons in the underlying spinor BEC model, we turn to numerical integration of the original GPEs (4) and (5). In particular, we first fix the value corresponding to  $^{23}\text{Na}$ ,  $\delta = 0.0314$  (we will consider different values of  $\delta$  in the following subsections), and use the following initial conditions for the densities:

$$|\psi_{\pm 1}(x,t=0)|^2 = \frac{1}{2}[\mu - \nu \operatorname{sech}^2(\sqrt{\nu}x)], \quad (34)$$

$$|\psi_0(x,t=0)|^2 = \frac{\nu^{3/2}\xi}{\eta\sqrt{\mu}} \operatorname{sech}^2(\sqrt{\nu}x). \quad (35)$$

Notice that the initial phase profiles are similar to those in Eqs. (28) and (29), while the parameter that determines the initial width of the soliton is

$$\nu \equiv 4\eta^2\delta. \quad (36)$$

Other parameters are chosen as  $\mu=2$ ,  $\xi=0.5$ , and  $\Omega_{\text{tr}}=0$  (for the homogeneous condensate), or  $\Omega_{\text{tr}}=0.05$  for the trapped condensate. In physical terms, this choice corresponds to the spinor condensate of sodium atoms with the peak 1D density  $n_0 \approx 10^8 \text{ m}^{-1}$ , which contains  $\approx 20\,000$  atoms confined in the trap with frequencies  $\omega_{\perp} = 34\omega_x = 2\pi \times 230 \text{ Hz}$ ; in this case, the time and space units are, respectively, 1.2 ms and 1.8  $\mu\text{m}$ .

Choosing the value  $\eta=1$  for the arbitrary parameter introduced above, and substituting  $\delta=0.0314$ ,  $\nu=0.13$ , we have checked that these values indeed provide for a very good agreement of the analytical predictions with numerical results. However, in this subsection, we will display numerical results obtained for an essentially larger value of  $\nu$ , viz.,  $\nu=1.2$ ; this choice, as seen from Eq. (36), corresponds to  $\eta=3.091$  and hence, from Eq. (34), to a soliton complex with deeper and narrower dark components and, accordingly, taller and narrower bright components. In this way, we intend to showcase the really wide range of validity of the analytical approach, and the robustness of the obtained solitary-wave solutions.

More specifically, we first check if the spinor DDB soliton complexes indeed behave as solitons, in the small-amplitude limit. To this end, we take initial conditions in the form of a superposition of two different pulses

$$\psi_{\pm 1}(x,0) = \sqrt{\frac{\mu}{2} - \frac{\nu}{2}[\operatorname{sech}^2(x_+) + \operatorname{sech}^2(x_-)]} \\ \times \exp\left(-i\sqrt{\frac{\nu}{\mu}}\tanh(x_+) + i\sqrt{\frac{\nu}{\mu}}\tanh(x_-)\right), \quad (37)$$

$$\psi_0(x,0) = \nu^{3/4} \sqrt{\frac{\xi}{\eta\sqrt{\mu}}} [\operatorname{sech}(x_+) e^{+i\sqrt{\mu}\nu x_+ - i(\xi/\eta)x_+} \\ + \operatorname{sech}(x_-) e^{-i\sqrt{\mu}\nu x_- + i(\xi/\eta)x_-}], \quad (38)$$

where  $x_{\pm} = \sqrt{\nu}(x \pm x_0)$  and  $x_0 = \pm 15$  are initial positions of centers of the two pulses. As seen in Eqs. (37) and (38), the soliton components are lent opposite initial momenta and, as a result, they propagate in opposite directions, as shown in the top panel of Fig. 1. We stress that even though a small amount of radiation is emitted in the course of the evolution (see four bottom panels of Fig. 1), the two dark solitons in the  $\psi_{\pm 1}$  fields, coupled to their bright counterparts in the  $\psi_0$  component, propagate practically undistorted, and around  $t=19$  they undergo a quasielastic collision; moreover, it is clearly observed that the solitons remain unscathed after the collision. This result is consistent with our asymptotic calculations performed above, indicating that the small-amplitude limit (for small  $\delta$ ) of the nonintegrable system of Eqs. (4) and (5) behaves similarly to the integrable YO system.

Next, we consider the confined system, with  $\Omega_{\text{tr}}=0.05$ . In this case, strictly speaking, the asymptotic reduction of Eqs. (4) and (5) to the YO system [Eqs. (24) and (27)] is not valid. Nevertheless, even in the presence of the external potential, the solutions obtained with  $\Omega_{\text{tr}}=0$  may be used as an initial configuration set near the bottom of the trap, to generate DDB- (or BBD-) like solutions of the inhomogeneous system. To that end, we first integrate Eqs. (4) and (5) in imaginary time, finding a ground state of the Thomas-Fermi (TF) type for fields  $\psi_{\pm 1}$ , which is approximated by the well-known analytical density profile [32]  $n_{\pm 1} = (1/2)(\mu - \Omega_{\text{tr}}^2 x^2)$ . Then, at  $t=0$ , the initial conditions for the  $\psi_{\pm 1}$  components are taken as the numerically found TF profiles multiplied by the dark soliton, as in Eq. (34), while the initial configuration of the  $\psi_0$  field is taken as the bright soliton in Eq. (35).

In such a case, and given that the spinor DDB solitons were found above to be robust objects behaving similarly to solitons of an integrable system, one may expect that the solitons would perform harmonic oscillations in the presence of the (sufficiently weak) parabolic trap. In fact, although this expectation sounds natural due to the large number of studies devoted to the dark soliton oscillations in inhomogeneous BECs, see below, the first works on this topic were surprising to many researchers. The earliest papers demonstrated that solitons oscillate in the single-component BEC confined in the harmonic traps of strength  $\Omega_{\text{tr}}$ , and provided estimates for the oscillation frequency. In particular, in Ref. [33] a soliton's equation of motion was presented without derivation, and it was stated that the solitons oscillate with frequency  $\Omega_{\text{tr}}$  (rather than  $\Omega_{\text{tr}}/\sqrt{2}$ ). The same was derived in Ref. [34] by considering the dipole mode of the condensate

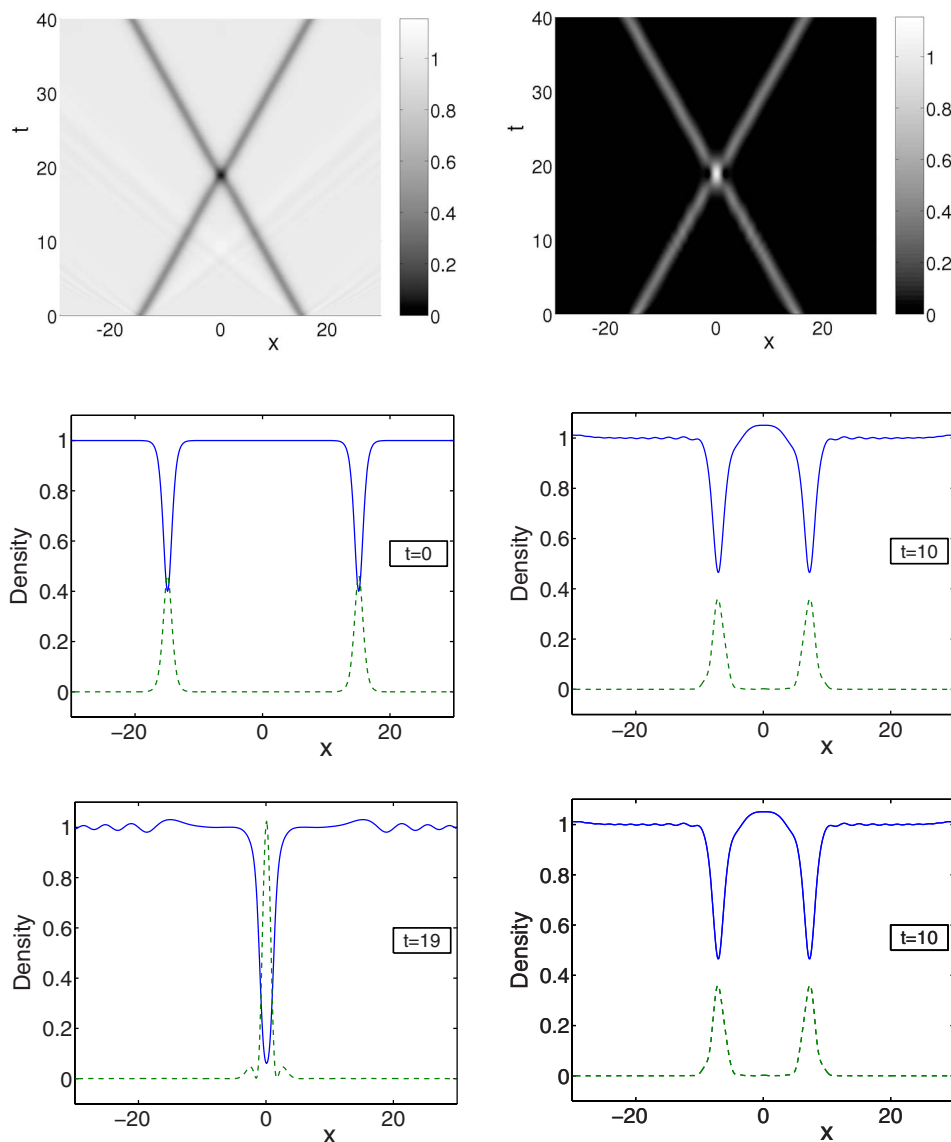


FIG. 1. (Color online) The two top panels show contour plots of the densities of the  $\psi_{\pm 1}$  (left panel) and  $\psi_0$  (right panel) components of the spinor condensate with  $\delta=0.0314$  in the homogeneous system ( $\Omega_{tr}=0$ ). The  $\psi_{\pm 1}$  components contain a pair of dark pulses, initially placed at  $x_0 = \pm 15$ , that, together with the bright components in the  $\psi_0$  field coupled to them, undergo a quasi-elastic collision at  $t \approx 19$ , and propagate unscathed afterward. The parameters are  $\mu=2$ ,  $\xi=1.54$ ,  $\eta=3.091$ , and  $\nu=1.2$ . The four bottom panels show snapshots of the densities observed at  $t=0, 10$  (before the collision),  $t=19$  (when the collision occurs), and  $t=40$  (after the collision).

supporting the dark soliton. Other works [35] also considered oscillations of dark solitons in such inhomogeneous single-component BECs. An analytical description of the dark-soliton motion and the correct result for the soliton oscillation frequency  $\Omega_{tr}/\sqrt{2}$  were first produced in Ref. [22] by means of a multiple-time-scale boundary-layer theory, and later by other analytical approaches [23]. Also, the motion of vector matter-wave solitons (of arbitrary amplitudes) in an harmonically confined two-component BEC was described analytically in Ref. [13].

Coming back to the present case, we find that, indeed, the DDB soliton complexes oscillate in the harmonically confined spinor BEC, as shown in Fig. 2. In particular, the DDB soliton, which was initially placed at the trap's center, oscillates as a whole without significant deformations of its components up to large times [while the figure extends to  $t=1000$  (which is 1.2 s in physical units), a similar behavior continues at still larger times]. This is a clear indication to the fact that the predicted DDB states have a good chance to be observed in the experiment. A noteworthy feature of the numerical data is that the bright-soliton component is guided

by the dark ones, the entire soliton complex oscillating at a single frequency. The value of the frequency is estimated below, for both small- and large-amplitude solitons.

### B. Oscillations of small-amplitude solitons

As mentioned above, various analytical techniques have been used to determine the soliton's oscillation frequency in harmonically trapped BECs, including multicomponent ones. In Ref. [13], the frequency was found analytically for solitons of arbitrary amplitude, and it was shown that in the special case of small-amplitude (shallow) solitons it is equal to  $\Omega_{tr}/\sqrt{2}$ , as in the case of single-component BECs [22,23]. However, the analysis in Ref. [13] was performed in the framework of the Manakov's system with the trapping potential, while here we are dealing with spinor condensates featuring nonzero spin-dependent interaction strength  $\delta$ , which implies a deviation from the Manakov type. Thus, our aim is, essentially, to extend the results of Ref. [13] to the case of nonzero  $\delta$  and present a semianalytical approach, valid for small-amplitude solitons (similar considerations,

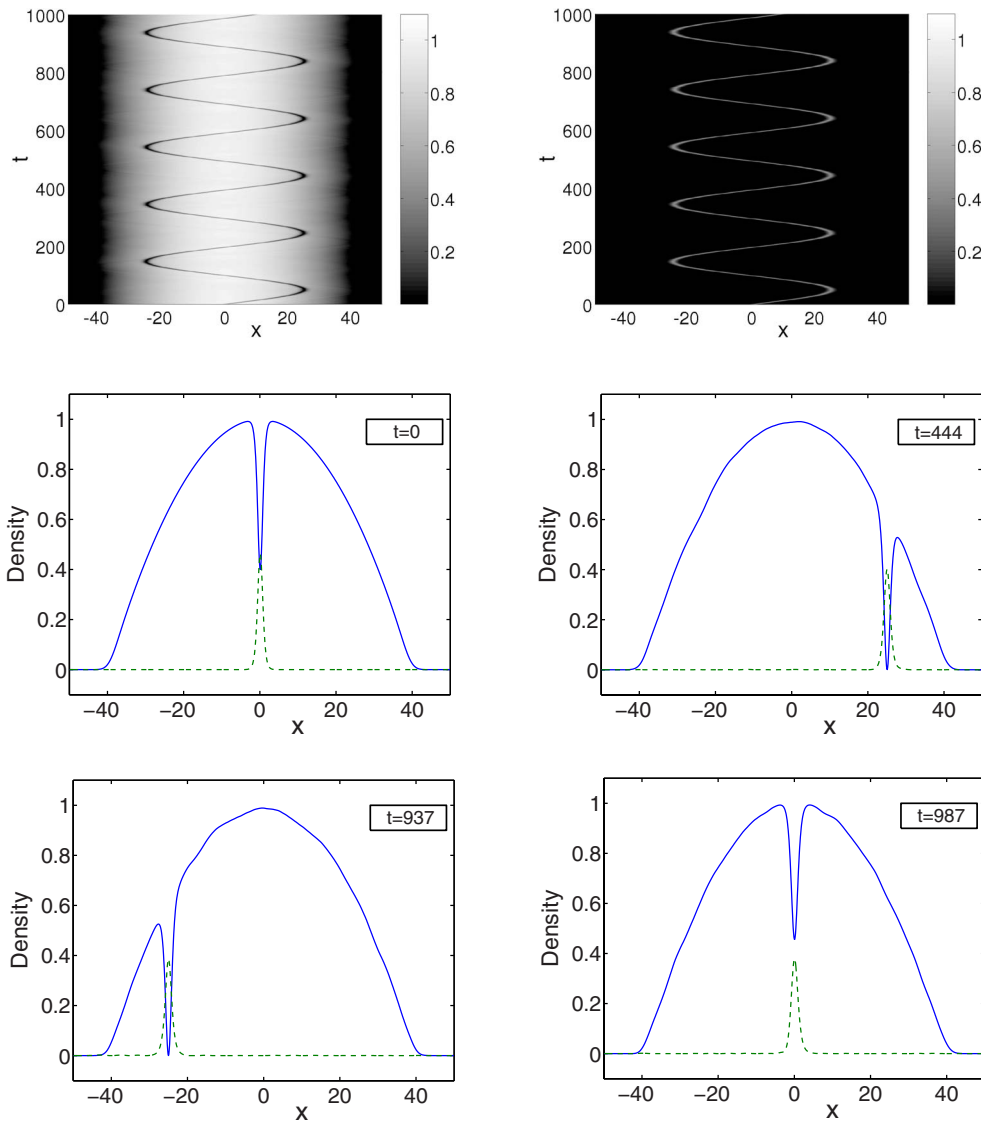


FIG. 2. (Color online) The two top panels show contour plots of the densities of the  $\psi_{\pm 1}$  (left) and  $\psi_0$  (right) fields confined in the harmonic trap with  $\Omega_{\text{tr}}=0.05$  (other parameters are the same as in Fig. 1). Initially, each of the Thomas-Fermi profiles of the  $\psi_{\pm 1}$  components carries a dark soliton, while the  $\psi_0$  component is a bright soliton (the initial position is at the trap's center  $x=0$ ). The four bottom panels show snapshots of the densities observed at  $t=0, 444, 937,$  and  $987$ .

but based on numerical simulations, will be presented for large-amplitude solitons in the next subsection).

We first consider the oscillations of small-amplitude solitons, assuming that  $\delta$  is small, with values  $0 < \delta \leq 10^{-1}$  (recall that  $\delta=0.0314$  corresponds to the spinor condensate of  $^{23}\text{Na}$  atoms). Then, to find the soliton oscillation frequency, we adopt what may be regarded as a local-density approximation (which is justified by the use of the asymptotic multiscale expansion method), similar to the one used in Refs. [36–38] for various scalar GPE-based models. This approximation assumes that the soliton velocity, which was found to be

$$\frac{dx}{dt} \equiv v = \sqrt{\mu} - 2\sqrt{\delta}\xi \quad (39)$$

in the homogeneous case [see Eq. (17)], will become spatially dependent in the inhomogeneous (harmonically confined) system, namely,

$$\frac{d\tilde{X}}{dt} = \tilde{v}(\tilde{X}), \quad (40)$$

where  $\tilde{X}$  is a properly chosen slow spatial variable (see below). Then, one has to determine the spatial dependence of the soliton velocity  $\tilde{v}(\tilde{X})$ , and solve the separable first-order differential equation (40) to determine the evolution of the soliton in the inhomogeneous system.

Following this approach, we first consider the simpler limiting case  $\delta \rightarrow 0$ . Then, Eq. (39) implies that the velocity of the small-amplitude soliton is approximately equal to the speed of sound, i.e.,  $v \approx c = \sqrt{\mu}$  [cf. Eq. (17)]. Accordingly, in the inhomogeneous system  $\tilde{v} \approx \tilde{c}(\tilde{X})$ , where  $\tilde{c}(\tilde{X})$  is the local speed of sound when the harmonic potential term,  $V = (1/2)\Omega_{\text{tr}}^2 x^2$  is included in the spin-independent part of the Hamiltonian  $\mathcal{H}_0$ . Then, taking into regard that the potential has little variation within the soliton size  $\sim \nu^{-1/2}$  (see, e.g., Fig. 2), we define the above-mentioned slow spatial variable as  $\tilde{X} = \tilde{\epsilon}x$ , where  $\tilde{\epsilon} = \Omega_{\text{tr}}/\tilde{\Omega}_{\text{tr}}$  [recall that  $\Omega_{\text{tr}}$  given in Eq. (6) is

of order  $10^{-2}$ ], and  $\tilde{\Omega}_{\text{tr}}$  is an auxiliary  $O(1)$  scale parameter. Then, the trapping potential takes the form of  $V(\tilde{X}) = (1/2)\tilde{\Omega}_{\text{tr}}^2\tilde{X}^2$ , i.e., it depends only on the slow variable  $\tilde{X}$ . The respective local speed of sound can easily be derived upon considering the linearization of Eqs. (11) and (12), which are modified by the inclusion of term  $-nV(\tilde{X})$  in the left-hand side of Eq. (11). The ground state of this system can easily be found by setting the atomic velocity  $v \equiv \phi_x = 0$  and  $\phi_t = -\mu$ . Then, since Eq. (11) implies that  $n = n_0$  is time independent in the ground state, we assume that  $n_0 = n_0(\tilde{X})$  and, to the leading order in  $\tilde{\epsilon}$ , we obtain

$$n_0(\tilde{X}) = (1/2)[\mu - V(\tilde{X})] \quad (41)$$

in the region where  $\mu > V(\tilde{X})$ , and  $n_0 = 0$  outside. Equation (41), which is the TF approximation for the density profile, also implies that, for  $V(\tilde{X}) = (1/2)\tilde{\Omega}_{\text{tr}}^2\tilde{X}^2$ , the axial size of the trapped condensate is  $2L \equiv 2\sqrt{2\mu}/\tilde{\Omega}_{\text{tr}}$ . Similarly to the analysis presented above in Sec. II B, we now consider the linearization around the ground state and seek respective solutions to Eqs. (11) and (12) as  $n = n_0(\tilde{X}) + \tilde{\epsilon}n_1(x, t)$ ,  $\phi = -\mu_0 t + \tilde{\epsilon}\phi_1(x, t)$ , and  $\Phi_0 = \tilde{\epsilon}\Phi_1(x, t)$ , with  $n_1, \phi_1, \Phi_1 \sim \exp[i(kx - \omega t)]$ . This way, we obtain the following dispersion relation for the inhomogeneous system  $\omega^2 = 2n_0(\tilde{X})k^2 + (1/4)k^4$  and, accordingly, the local speed of sound:

$$\tilde{c}(\tilde{X}) = \sqrt{2n_0(\tilde{X})}, \quad (42)$$

which bears resemblance to the sound propagation in weakly nonuniform media [39]; in the homogeneous case, Eq. (42) is reduced to Eq. (17). Next, recalling that  $\tilde{v}(\tilde{X}) \approx \tilde{c}(\tilde{X})$  (for  $\delta = 0$ ), we substitute Eq. (42) in Eq. (40) and, taking into regard the density profile given by Eq. (41), we integrate the resulting first-order differential equation to obtain

$$\tilde{X} = L \sin(\omega_{\text{osc}} t), \quad (43)$$

where  $\omega_{\text{osc}} = \Omega_{\text{tr}}/\sqrt{2}$  (for the sake of simplicity, we dropped the tilde in  $\Omega_{\text{tr}}$ ). Thus, for  $\delta = 0$ , we recover the known result for the oscillations of dark solitons in single-component [22,23] and two-component BECs [13] (in the small-amplitude limit).

Next, we consider the case of nonzero (but small)  $\delta$ . To determine the soliton oscillation frequency via Eq. (40) in this case, one should again substitute  $\mu \rightarrow 2n_0(\tilde{X}) = \mu - (1/2)\tilde{\Omega}_{\text{tr}}^2\tilde{X}^2$  in Eq. (39), and additionally find the spatial dependence of the soliton parameter  $\xi$ . The latter will also become a function of  $\tilde{X}$  in the inhomogeneous case, which, in principle, may be determined upon analyzing the inhomogeneous YO system (similar to how it was done, e.g., in Refs. [36–38] in the context of the inhomogeneous Korteweg–de Vries equation). Here, we will follow a simpler approach and use numerical simulations to approximate the soliton velocity  $\tilde{v}$  as a function of  $\tilde{X}$ . Thus, fixing the value of the soliton amplitude (we have used  $\nu/\mu = 0.15$ ), we numerically integrate GPEs (4) and (5) for values of  $\delta$  from interval  $0 < \delta \leq 0.1$  to determine  $\tilde{v}(X)$ . The result is

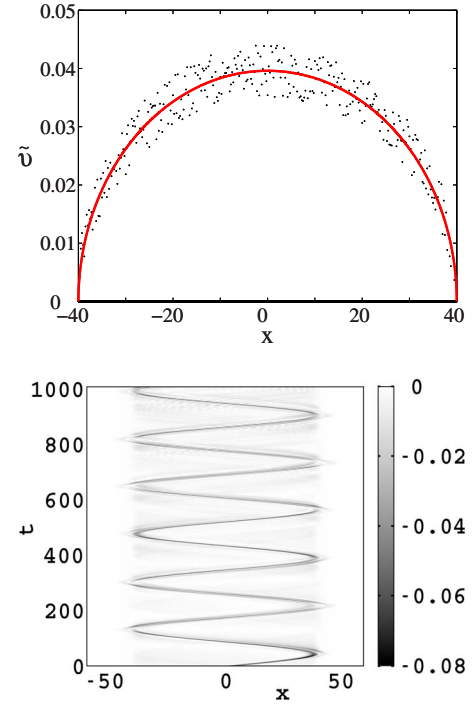


FIG. 3. (Color online) Top panel: The spatial dependence of the soliton velocity  $\tilde{v}$  for  $\delta = 0.0314$ . Dots correspond to results produced by the numerical simulations, while the (red) solid line represents the best fit, which is found to be  $0.028\sqrt{2n_0(X)} = 0.028\sqrt{\mu - (1/2)\tilde{\Omega}_{\text{tr}}^2\tilde{X}^2}$  (the values of the chemical potential and trap's strength are  $\mu = 2$  and  $\tilde{\Omega}_{\text{tr}} = 0.05$ , as before). Bottom panel: Contour plots of the effective density of the shallow dark soliton  $|\psi_{\pm}|^2 - 2n_0(X)$  for  $\delta = 0.0314$ , with initial amplitude  $\nu = 0.13$ ; the other parameters are  $\eta = 1$ ,  $\xi = 0.5$ ,  $\mu = 2$ , and  $\tilde{\Omega}_{\text{tr}} = 0.05$ . The soliton performs oscillations at frequency  $\omega_{\text{osc}} \approx 0.03433$ , which is almost identical to the analytical prediction  $\Omega_{\text{osc}} = 0.0344$  (the error is  $\approx 0.24\%$ ).

$$\tilde{v}(\tilde{X}) = A(\delta)\sqrt{2n_0(\tilde{X})}, \quad (44)$$

$$A(\delta) = \alpha\sqrt{\delta} + \beta, \quad (45)$$

with  $\alpha = 0.151$  and  $\beta = 0.0029$ . An example of such a numerical estimation of the spatial dependence of the soliton velocity is shown in the left panel of Fig. 3 for  $\delta = 0.0314$  (notice that  $\tilde{v}$  is computed as a function of  $x$  which implicitly defines it as a function of  $\tilde{X}$ ); in this case, the best fit [depicted by the (red) solid line] corresponding to the numerically found values of  $\tilde{v}$  (depicted by the sparse points) is  $0.028\sqrt{2n_0(\tilde{X})}$ . Notice that, since  $\mu \rightarrow 2n_0(\tilde{X})$  and  $\tilde{v} \sim \sqrt{2n_0(\tilde{X})}$ , Eq. (39) implies that, in the inhomogeneous case,  $\xi(x) \sim \sqrt{2n_0(\tilde{X})}$ .

Having found the spatial dependence of the soliton velocity, we may substitute expressions (44) and (45) in Eq. (40), integrate the resulting equation, and again obtain Eq. (43), but with the soliton oscillation frequency as a function of  $\delta$ :

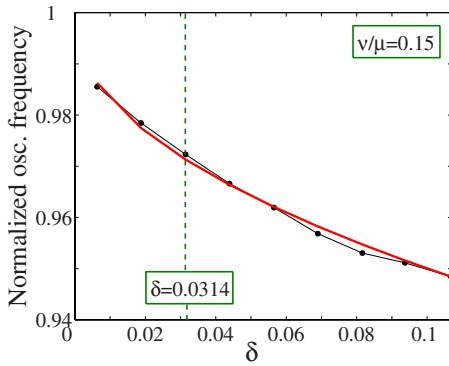


FIG. 4. (Color online) The oscillation frequency of the small-amplitude spinor DDB soliton (with  $\nu/\mu=0.15$ ) normalized to the characteristic value  $\Omega_{\text{tr}}/\sqrt{2}$  as a function of  $\delta$ . The thick (red) solid line corresponds to the semianalytical prediction given by Eq. (46), while the piecewise linear line (black) with dots represents results obtained by the direct numerical integration of the Gross-Pitaevskii Eqs. (4) and (5). The vertical dotted line indicates the value of  $\delta=0.0314$  corresponding to the  $^{23}\text{Na}$  spinor BEC.

$$\omega_{\text{osc}} = \frac{\Omega_{\text{tr}}}{\sqrt{2}}(1 - \alpha\sqrt{\delta}) - \epsilon, \quad (46)$$

where  $\epsilon \equiv \beta\Omega_{\text{tr}}/\sqrt{2}$  (for  $\Omega_{\text{tr}}=0.05$ , we have  $\epsilon \approx 10^{-4}$ ). Apparently, for  $\delta=0$ , we recover the result obtained above, i.e.,  $\omega_{\text{osc}}=\Omega_{\text{tr}}/\sqrt{2}$ . Thus, it is clear that Eq. (46) generalizes the result first presented in Ref. [13] for two-component BECs  $\omega_{\text{osc}}=\Omega_{\text{tr}}/\sqrt{2}$ , to the case of spinor condensates with nonzero spin-dependent interaction strength  $\delta$ . Note that the oscillation frequency is down-shifted, as compared to the value of  $\Omega_{\text{tr}}/\sqrt{2}$ , i.e., the dark-bright pair executes slower oscillations as the spin-dependent interaction strength is increased. However, it should be stressed that the above results [Eqs. (43) and (46)] are valid for the shallow solitons, with relative depth  $\nu/\mu \ll 1$ ; see Eq. (34).

The above estimates have been tested against direct numerical integration of GPEs (4) and (5), using as initial condition a sufficiently shallow DDB soliton. First, we present a specific example (see right panel of Fig. 3) of such a shallow soliton with  $\nu/\mu=0.065$ , which corresponds to the above-mentioned physically relevant choice of  $\nu=0.13$  and chemical potential  $\mu=2$ . In this case, the analytical prediction is quite accurate, as the numerically found oscillation frequency for  $\delta=0.0314$  and  $\Omega_{\text{tr}}=0.05$  is  $\approx 0.03433$ , while the analytical prediction of Eq. (46) is 0.0344, the respective error being just  $\approx 0.24\%$ . On the other hand, as seen in the same figure, the amplitude of the soliton oscillations is 39.992, while the prediction is  $L=\sqrt{2}\mu/\Omega=40$  as per Eq. (43); here, the error is 0.02%.

Next, we fix the soliton amplitude, taking  $\nu/\mu=0.15$ , and vary  $\delta$  to check the accuracy of the semianalytical approach presented above. As seen in Fig. 4, the numerically found oscillation frequency (the piecewise-linear line with the dots) is observed to be in excellent agreement with the semianalytical result given by Eq. (46) [the thick (red) solid line]; in fact, the values of  $\alpha$  and  $\epsilon$  were found to be 0.153 (instead of 0.151) and  $5.5 \times 10^{-5}$  (instead of  $10^{-4}$ ), respectively. Note

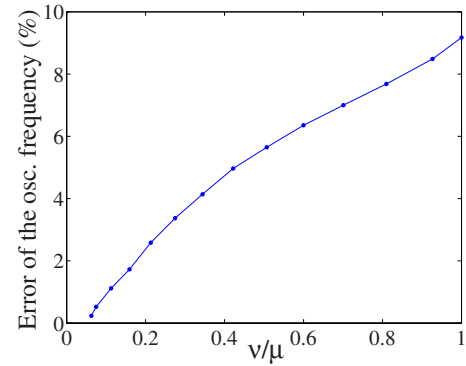


FIG. 5. (Color online) The relative deviation of the numerically found soliton oscillation frequency from the value predicted by Eq. (46), as a function of the relative dark-soliton depth  $\nu/\mu$  for  $\delta=0.0314$ . The region of  $\nu/\mu \ll 1$  corresponds to shallow solitons, while  $\nu/\mu=1$  corresponds to a black soliton. It is seen that the analytical prediction is fairly good for shallow solitons (for  $\nu/\mu < 0.4$ , the error is below 5%), but becomes worse for the solitons with moderate and large amplitudes (for  $\nu/\mu > 0.8$ , the error becomes  $\sim 10\%$ ).

that the value of error  $\epsilon$  found numerically by means of the GPE model is smaller than the semianalytical prediction given by Eq. (46), as the numerical scheme for the determination of the soliton oscillation frequency is much more accurate than the one used for the determination of the spatial dependence of the soliton velocity.

### C. Oscillations of moderate- and large-amplitude solitons

It is necessary to compare the predictions for the oscillations of the solitons given by Eqs. (43) and (46) to results of direct simulations, including those for the solitons with moderate and large amplitudes. To this end, in Fig. 5 we show the relative discrepancy between the numerically found soliton oscillation frequency and the prediction produced by Eq. (46) as a function of the relative dark-soliton's depth  $\nu/\mu$  for  $\delta=0.0314$ . The region of  $\nu/\mu \ll 1$  corresponds to shallow solitons, while the limiting case of  $\nu/\mu=1$  represents the “black” soliton, with the initial intensity at the soliton center set equal to zero (the latter is slightly displaced from the trap's center to initiate the motion). As seen in the figure, the prediction provided by Eq. (46) is very good for every  $\nu/\mu < 0.2$ , as the relative error in the frequency is below 2%. We have also computed the error in the oscillation amplitude (not shown here), which we have found to be larger (up to 17% in this regime of  $\nu/\mu < 0.2$ ); this is due to the fact that the increasingly deeper solitons are not reflected at the rims of the condensate, but rather inside the cloud, as can be seen, e.g., in Fig. 2.

For the solitons with moderate and large amplitudes, the analytical prediction is worse. For example, in the case shown in Fig. 2 (with  $\nu/\mu=0.6$ ), comparing the numerically found soliton oscillation frequency  $\omega_{\text{osc}} \approx 0.032$  to the above-mentioned predicted value 0.0344 (again for  $\Omega_{\text{tr}}=0.05$ ), we find a relatively large discrepancy ( $\approx 7\%$ ) between them. However, an important observation regarding Fig. 2, which

is true also for DDB solitons of an arbitrary amplitude, is that the bright-soliton component performs oscillations at the same frequency as its dark counterpart. This is a clear indication of the fact that the bright component is guided (being effectively trapped) by the dark component of the DDB complex. Note that in the single-component BEC, bright solitons oscillate in the parabolic potential with a different frequency, namely,  $\Omega_{\text{tr}}$  [24] (which is a consequence of the Kohn's theorem [25]).

Naturally, the discrepancy becomes larger in the case of large-amplitude (nearly black) solitons, which perform small-amplitude oscillations around the trap's center. For example, for  $\nu/\mu=0.8$  ( $\nu/\mu=0.9$ ) the numerically found values of the oscillation frequency deviate from those predicted by Eq. (46) by 7.7% (8.4%), while in the limiting case of  $\nu/\mu=1$  the respective error is 9.2%. The deviations are due to the fact that the numerical results pertain to solitons with large values of  $\nu/\mu$ , while the analytical approach was developed under the assumption of  $\nu/\mu \ll 1$ , as said above.

In the case of large-amplitude solitons, it is relevant to compare the numerically found oscillation frequency to a different analytical prediction presented in Ref. [13]. In that work, the oscillation frequency was obtained from a nonlinear equation of motion for the bright-dark vector soliton in a binary BEC mixture [Eq. 5 of Ref. [13]]. In fact, for shallow solitons the oscillation frequency is the same as above  $\omega_{\text{osc}} = \Omega_{\text{tr}}/\sqrt{2}$ , while, in the opposite limit of very deep dark solitons, it is approximated (in terms of the present notation) by the expression

$$\Omega_{\text{osc}} = \frac{\Omega_{\text{tr}}}{\sqrt{2}} \left( 1 - \frac{N_B}{4\sqrt{\mu + (N_B/4)^2}} \right)^{1/2}, \quad (47)$$

where  $N_B$  is the number of atoms of the bright-soliton component. The latter, employing Eq. (35), is easily found to be  $N_B = 2\nu^{3/2}\xi/\eta\sqrt{\mu}$  or

$$N_B = \mu(\nu/\mu)^{3/2}. \quad (48)$$

According to Eq. (47), the oscillation frequency is down-shifted as compared to the value of  $\Omega_{\text{tr}}/\sqrt{2}$  (i.e., the dark-bright pair executes slower oscillations, as the bright component is enhanced), in agreement with our numerical observations. In particular, for normalized soliton depths  $\nu/\mu=0.8, 0.9, 0.95$ , and 1, the values given by Eq. (47) deviate from the numerically found frequencies by 1.7, 4, 4.6, and 5.2 %, respectively.

On the other hand, as seen from Eq. (48), the norm of the bright component  $N_B$  does not depend on the strength of the spin-sensitive interaction; this fact implies that the oscillation frequency of large-amplitude solitons given by Eq. (47) does not depend on  $\delta$ . However, the results reported above for small-amplitude solitons suggest that the oscillation frequency depends on  $\delta$ . Results obtained from the direct numerical integration of GPEs (4) and (5) reveal that this is the case indeed: the actual oscillation frequency can be very well approximated by the following fitting formula:

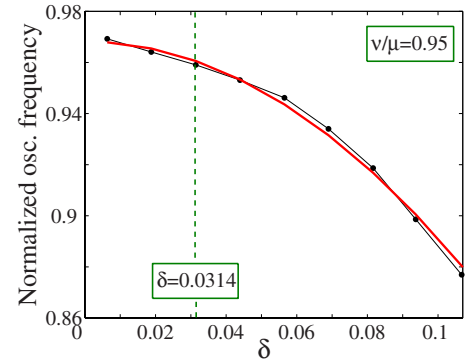


FIG. 6. (Color online) The oscillation frequency of the large-amplitude spinor DDB (dark-dark-bright) soliton, with  $\nu/\mu=0.95$ , normalized to the value  $\Omega_{\text{osc}}$  given in Eq. (47), as a function of  $\delta$ . The piecewise linear line (black) with dots represents the results obtained by the direct numerical integration of Eqs. (4) and (5), while the thick (red) solid line depicts the best fit based on Eq. (49). The vertical dashed line indicates the value of  $\delta=0.0314$  corresponding to the spinor BEC in  $^{23}\text{Na}$ .

$$\omega_{\text{osc}} = \Omega_{\text{osc}}(1 - \alpha_0\delta^2) - \epsilon_0, \quad (49)$$

where  $\Omega_{\text{osc}}$  is given by Eq. (47), while constants  $\alpha_0$  and  $\epsilon_0$  depend on the normalized soliton amplitude  $\nu/\mu$ . In particular, we have found that for  $\nu/\mu=0.95$ , these values are  $\alpha_0 = 7.71$  and  $\epsilon_0 = 9.3 \times 10^{-4}$ . The respective result is shown in Fig. 6, where the oscillation frequency [normalized to the value given by Eq. (47)] is shown as a function of  $\delta$ . It is seen that, similar to the case of small-amplitude solitons, the oscillation frequency, which may be approximated by Eq. (49), is down-shifted against the value given by Eq. (47), i.e., the dark-bright complex executes slower oscillations as the spin-dependent interaction strength increases. Apparently, this generalization of the result obtained in Ref. [13], indicates that an analytical investigation of the motion of bright-dark soliton complexes (of arbitrary amplitudes) in the trapped spinor condensate would be very relevant. However, such a detailed study is beyond the scope of the present work.

#### D. Effects of stronger spin-dependent interaction

In the previous subsections we dealt with small values of  $\delta$ , based on the fact that  $\delta=0.0314$  corresponds to the polar spin-1 BEC in sodium. Such small values of  $\delta$  validate the perturbative approach, which allowed us to find approximate DDB soliton solutions of the YO type, and study their oscillations in the trapped spinor condensate. It is interesting, however, to test the stability and dynamics of the DDB solitons in the more general case of nonsmall values of  $\delta$ . In this respect, we will here present numerical results obtained by the direct numerical integration of Eqs. (4) and (5) for  $\delta=0.2$  (which is an order of magnitude greater than the previous value). We will consider the evolution of DDB solitons with the same amplitudes as in the case of small  $\delta$ , so as to directly compare the results pertaining to weak and moderate spin-dependent interaction strengths.

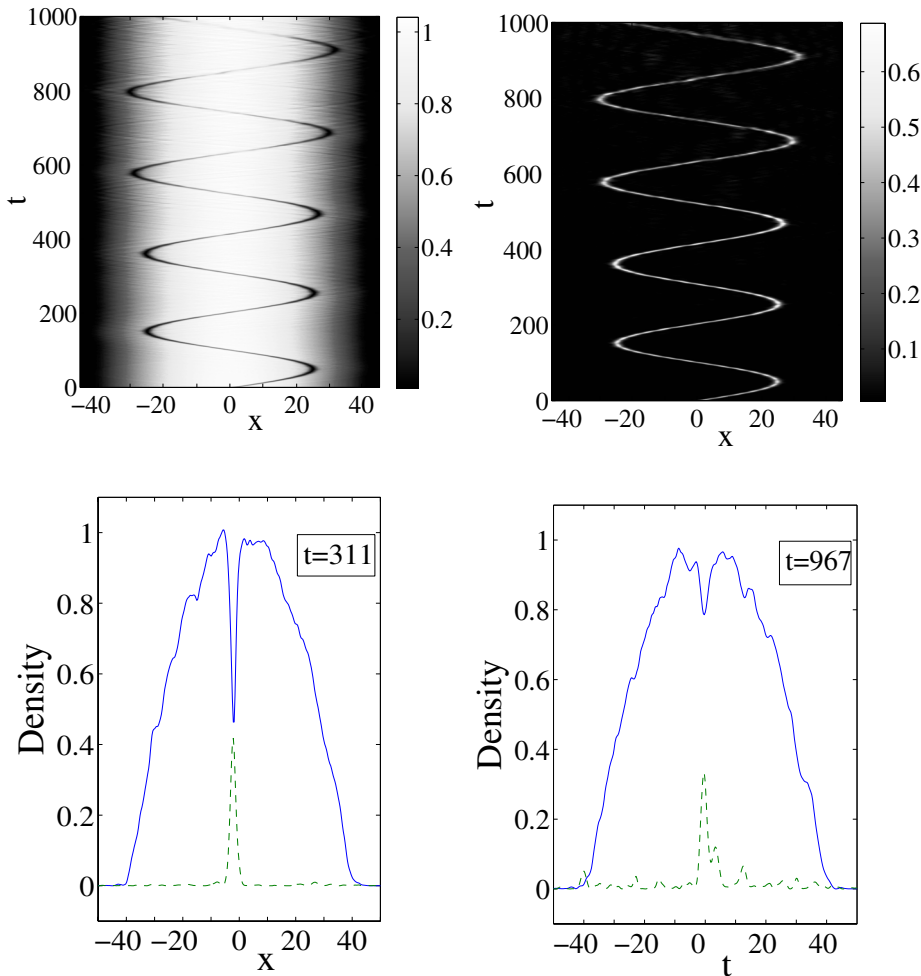


FIG. 7. (Color online) Same as Fig. 2, but for  $\delta=0.2$ . The soliton parameters are  $\xi=0.61$ ,  $\eta=1.22$ , and  $\nu=1.2$ , while the trap strength and chemical potential are  $\Omega_{\text{tr}}=0.05$  and  $\mu=2$ . This choice makes the initial soliton densities identical to those shown in the second-row left panel of Fig. 2. The two bottom panels are snapshots of the densities at  $t=311$  and 967.

In Fig. 7, we show the evolution of a DDB soliton with a moderate amplitude, characterized by parameters  $\xi=0.61$ ,  $\eta=1.22$ , and  $\nu=1.2$ , for the same values of the trap strength and chemical potential as before ( $\Omega_{\text{tr}}=0.05$  and  $\mu=2$ ), and the same initial condition as that in the second-row left panel of Fig. 2 (recall that, in this case, the normalized amplitude of the dark solitons in the  $\psi_{\pm 1}$  components is  $\nu/\mu=0.6$ ). As observed in Fig. 7, although the stronger perturbation induces emission of stronger radiation (as seen in the bottom left panel), the loss is not significant up to relatively large times, such as  $t=311$  (or  $t=360$  ms, in physical units): the density in the dark (bright) soliton is only 8% (9%) smaller than its initial values. Thus, one may conclude that even for such a large value of  $\delta$  the DDB vector soliton has a good chance to be observed in an experiment (provided, of course, that the respective magnitude of the spin-dependent interaction is achievable in the experiment). However, at still later times the continuous perturbation-induced emission of radiation results in eventual destruction of the DDB complex. In particular, at  $t=967$  (see the bottom right panel of Fig. 7), the density in the dark (bright) soliton is 63% (28%) smaller than the initial value.

The large- and small-amplitude solitons, with normalized amplitudes (of the dark soliton)  $\nu/\mu=0.8$  and  $\nu/\mu=0.065$ , respectively, were examined too (results not shown here). It was found that, naturally, the large-amplitude DDB soliton starts to accelerate immediately due to the strong emission of

radiation and quickly decays, being destroyed at  $t \approx 300$ , when densities in it fall below half of their initial values. On the other hand, the small-amplitude DDB soliton was found to be slightly more robust, featuring a behavior similar to that of the moderate-amplitude soliton in Fig. 4, but at shorter times: the vector soliton persists up to  $t \approx 600$  (when the densities become smaller than 50% of their initial values), and then decays. Thus, it may be inferred that the small- and moderate-amplitude YO-type DDB vector solitons persist in the spin-1 condensate up to experimentally relevant times even for strong spin-dependent interaction, with the strength an order of magnitude larger than the actual value for the polar spinor condensate in sodium.

#### IV. CONCLUSIONS

We have studied bright-dark soliton complexes in polar spinor Bose-Einstein condensates, both analytically and numerically. Our analytical approach is based on the small-amplitude asymptotic reduction of the nonintegrable vectorial (three-component) system of the coupled Gross-Pitaevskii equations to a completely integrable model, viz., the Yajima-Oikawa system. Borrowing soliton solutions of the Yajima-Oikawa system and inverting the reduction, we have obtained an analytical approximation for small-amplitude vector solitons of the dark-dark-bright and bright-bright-dark types, in terms of the  $m_F = +1, -1, 0$  components,

respectively. The analytical predictions were confirmed by direct numerical simulations. The so constructed approximate soliton states were found to propagate undistorted and undergo quasielastic collisions, featuring properties of genuine solitons.

Effects of the harmonic trapping potential (which also contributes toward the nonintegrability of the underlying equations) on the solitons were also studied numerically and analytically. It was found that even vector solitons with moderate (nonsmall) amplitudes maintain their identity in the presence of the parabolic trap, and perform harmonic oscillations, up to long times ( $\geq 10$  s, in physical units).

We have studied in detail the oscillations of the vector solitons of small, moderate, and large amplitudes. In the former case, and for a sufficiently small normalized strength of the spin-dependent interaction  $\delta$ , we used a semianalytical technique (based on the local-density approximation) to arrive at the following conclusions: the soliton oscillation frequency is down-shifted (as compared to the value of  $\Omega_{tr}/\sqrt{2}$  found in Ref. [13] for a binary BEC), i.e., the dark-bright soliton pair executes slower oscillations, as the spin-dependent interaction strength increases, with the shift growing as  $\sqrt{\delta}$ . It was found that, for the initial soliton depth below 10% of the chemical potential, the deviation of the analytical prediction from the numerically found oscillation frequency was below 1% (the error in the estimate of the amplitude of the soliton oscillation was below 8%). For the moderate- and large-amplitude solitons, the discrepancy in the frequency was larger ( $\sim 10\%$ ); however, in the case of very deep dark solitons we have checked that the respective prediction of Ref. [13] leads to a significantly smaller error  $< 5\%$ . In the latter case, we have found numerically that

(similarly to the case of small-amplitude solitons) the oscillation frequency again gets down-shifted (as compared to the prediction of Ref. [13]) as the spin-dependent interaction strength increases, but now proportional to  $\delta^2$ . Our results indicate that an elaborated analytical description of the bright-dark soliton motion (for solitons of an arbitrary amplitude) in the trapped spinor condensate is a challenge for future work.

We also tested the robustness of the derived vector soliton solutions in the case of a large normalized strength of the spin-dependent interaction, an order of magnitude larger than the value corresponding to the polar spinor condensate in sodium. We have found that, although the solitons eventually get destroyed under such a strong perturbation, the lifetime of small- and moderate-amplitude DDB solitons exceeds 300 ms, in physical units. Thus, the vector solitons predicted in this work have a good chance to be observed in experiments.

The bright-soliton component(s) were found to be guided by their dark counterpart(s), oscillating with the frequency determined by the dark components. This is an example of the all-matter-wave soliton guidance, with potential applications in the design of quantum switches and splitters.

#### ACKNOWLEDGMENTS

The work of H.E.N. and D.J.F. was partially supported by the Special Research Account of the University of Athens. H.E.N. acknowledges partial support from EC grants PYTHAGORAS-I. The work of B.A.M. was supported, in part, by the Israel Science Foundation through the Center-of-Excellence Grant No. 8006/03, and German-Israel Foundation (GIF) Grant No. 149/2006.

- 
- [1] D. M. Stamper-Kurn and W. Ketterle, e-print arXiv:cond-mat/0005001.
- [2] D. M. Stamper-Kurn, M. R. Andrews, A. P. Chikkatur, S. Inouye, H.-J. Miesner, J. Stenger, and W. Ketterle, *Phys. Rev. Lett.* **80**, 2027 (1998).
- [3] M.-S. Chang, C. D. Hamley, M. D. Barrett, J. A. Sauer, K. M. Fortier, W. Zhang, L. You, and M. S. Chapman, *Phys. Rev. Lett.* **92**, 140403 (2004).
- [4] J. Stenger, S. Inouye, D. M. Stamper-Kurn, H.-J. Miesner, A. P. Chikkatur, and W. Ketterle, *Nature (London)* **396**, 345 (1998).
- [5] A. E. Leanhardt, Y. Shin, D. Kielpinski, D. E. Pritchard, and W. Ketterle, *Phys. Rev. Lett.* **90**, 140403 (2003).
- [6] J. Ieda, T. Miyakawa, and M. Wadati, *Phys. Rev. Lett.* **93**, 194102 (2004); J. Ieda, T. Miyakawa, and M. Wadati, *J. Phys. Soc. Jpn.* **73**, 2996 (2004).
- [7] L. Li, Z. Li, B. A. Malomed, D. Mihalache, and W. M. Liu, *Phys. Rev. A* **72**, 033611 (2005).
- [8] W. Zhang, Ö. E. Müstecaplıoglu, and L. You, *Phys. Rev. A* **75**, 043601 (2007).
- [9] M. Uchiyama, J. Ieda, and M. Wadati, *J. Phys. Soc. Jpn.* **75**, 064002 (2006).
- [10] B. J. Dabrowska-Wüster, E. A. Ostrovskaya, T. J. Alexander, and Y. S. Kivshar, *Phys. Rev. A* **75**, 023617 (2007).
- [11] Yu. S. Kivshar and G. P. Agrawal, *Optical Solitons: From Fibers to Photonic Crystals* (Academic Press, New York, 2003).
- [12] B. Luther-Davies and X. Yang, *Opt. Lett.* **17**, 496 (1992).
- [13] Th. Busch and J. R. Anglin, *Phys. Rev. Lett.* **87**, 010401 (2001).
- [14] S. V. Manakov, *Zh. Eksp. Teor. Fiz.* **65**, 505 (1973) [*Sov. Phys. JETP* **38**, 248 (1974)].
- [15] E. G. M. van Kempen, S. J. J. M. F. Kokkelmans, D. J. Heinzen, and B. J. Verhaar, *Phys. Rev. Lett.* **88**, 093201 (2002).
- [16] N. N. Klausen, J. L. Bohn, and C. H. Greene, *Phys. Rev. A* **64**, 053602 (2001).
- [17] V. E. Zakharov and S. V. Manakov, *Zh. Eksp. Teor. Fiz.* **71**, 203 (1976) [*Sov. Phys. JETP* **42**, 842 (1976)]; V. E. Zakharov and E. I. Schulman, *Physica D* **4**, 270 (1982); V. G. Makhan'kov and O. K. Pashaev, *Theor. Math. Phys.* **53**, 979 (1982).
- [18] N. Yajima and M. Oikawa, *Prog. Theor. Phys.* **56**, 1719 (1976).
- [19] Y. S. Kivshar, *Opt. Lett.* **17**, 1322 (1992).
- [20] M. Aguero, D. J. Frantzeskakis, and P. G. Kevrekidis, *J. Phys. A* **39**, 7705 (2006).
- [21] N. P. Robins, W. Zhang, E. A. Ostrovskaya, and Y. S. Kivshar,

- Phys. Rev. A **64**, 021601(R) (2001).
- [22] Th. Busch and J. R. Anglin, Phys. Rev. Lett. **84**, 2298 (2000).
- [23] D. J. Frantzeskakis, G. Theocharis, F. K. Diakonos, P. Schmelcher, and Yu. S. Kivshar, Phys. Rev. A **66**, 053608 (2002); V. V. Konotop and L. Pitaevskii, Phys. Rev. Lett. **93**, 240403 (2004); G. Theocharis, P. Schmelcher, M. K. Oberthaler, P. G. Kevrekidis, and D. J. Frantzeskakis, Phys. Rev. A **72**, 023609 (2005); D. E. Pelinovsky, D. J. Frantzeskakis, and P. G. Kevrekidis, Phys. Rev. E **72**, 016615 (2005).
- [24] U. Al Khawaja, H. T. C. Stoof, R. G. Hulet, K. E. Strecker, and G. B. Partridge, Phys. Rev. Lett. **89**, 200404 (2002); P. G. Kevrekidis, D. J. Frantzeskakis, R. Carretero-González, B. A. Malomed, G. Herring, and A. R. Bishop, Phys. Rev. A **71**, 023614 (2005).
- [25] W. Kohn, Phys. Rev. **123**, 1242 (1961); J. F. Dobson, Phys. Rev. Lett. **73**, 2244 (1994).
- [26] M. Moreno-Cardoner, J. Mur-Petit, M. Guilleumas, A. Polls, A. Sanpera, and M. Lewenstein, Phys. Rev. Lett. **99**, 020404 (2007); J. Mur-Petit, M. Guilleumas, A. Polls, A. Sanpera, M. Lewenstein, K. Bongs, and K. Sengstock, Phys. Rev. A **73**, 013629 (2006).
- [27] V. M. Pérez-García, H. Michinel, and H. Herrero, Phys. Rev. A **57**, 3837 (1998).
- [28] T.-L. Ho, Phys. Rev. Lett. **81**, 742 (1998).
- [29] T. Ohmi and K. Machida, J. Phys. Soc. Jpn. **67**, 1822 (1998).
- [30] H. Pu, C. K. Law, S. Raghavan, J. H. Eberly, and N. P. Bigelow, Phys. Rev. A **60**, 1463 (1999); H. Pu, S. Raghavan, and N. P. Bigelow, *ibid.* **61**, 023602 (2000).
- [31] S. Yi, Ö. E. Müstecaplıoğlu, C. P. Sun, and L. You, Phys. Rev. A **66**, 011601(R) (2002); H. E. Nistazakis, D. J. Frantzeskakis, P. G. Kevrekidis, B. A. Malomed, R. Carretero-González, and A. R. Bishop, *ibid.* **76**, 063603 (2007).
- [32] L. P. Pitaevskii and S. Stringari, *Bose-Einstein Condensation* (Oxford University Press, Oxford, 2003).
- [33] W. P. Reinhardt and C. W. Clark, J. Phys. B **30**, L785 (1997).
- [34] S. A. Morgan, R. J. Ballagh, and K. Burnett, Phys. Rev. A **55**, 4338 (1997).
- [35] A. D. Jackson, G. M. Kavoulakis, and C. J. Pethick, Phys. Rev. A **58**, 2417 (1998); T. Hong, Y. Z. Wang, and Y. S. Huo, *ibid.* **58**, 3128 (1998); X.-J. Chen, J.-Q. Zhang, and H.-C. Wong, Phys. Lett. A **268**, 306 (2000).
- [36] G. Huang, J. Szeftel, and S. Zhu, Phys. Rev. A **65**, 053605 (2002).
- [37] D. J. Frantzeskakis, N. P. Proukakis, and P. G. Kevrekidis, Phys. Rev. A **70**, 015601 (2004).
- [38] D. J. Frantzeskakis, P. G. Kevrekidis, and N. P. Proukakis, Phys. Lett. A **364**, 129 (2007).
- [39] L. D. Landau and E. M. Lifshitz, *Fluid Mechanics* (Pergamon, New York, 1959).